Structural and Dynamic Analysis of Residual Dipolar Coupling Data for Proteins

Joel R. Tolman,*,†,|| Hashim M. Al-Hashimi,‡,§ Lewis E. Kay,† and James H. Prestegard§

Contribution from the Protein Engineering Network Centers of Excellence, and the Departments of Medical Genetics, Biochemistry and Chemistry, University of Toronto, Toronto, Ontario, Canada M5S 1A8, Department of Chemistry, Yale University, New Haven, Connecticut 06511, and Complex Carbohydrate Research Center, University of Georgia, Athens, Georgia 30602

Received July 10, 2000. Revised Manuscript Received November 6, 2000

Abstract: The measurement of residual dipolar couplings in weakly aligned proteins can potentially provide unique information on their structure and dynamics in the solution state. The challenge is to extract the information of interest from the measurements, which normally reflect a convolution of the structural and dynamic properties. We discuss here a formalism which allows a first order separation of their effects, and thus, a simultaneous extraction of structural and motional parameters from residual dipolar coupling data. We introduce some terminology, namely a generalized degree of order, which is necessary for a meaningful discussion of the effects of motion on residual dipolar coupling measurements. We also illustrate this new methodology using an extensive set of residual dipolar coupling measurements made on $^{15}N,^{13}C$-labeled human ubiquitin solvated in a dilute bicelle solution. Our results support a solution structure of ubiquitin which on average agrees well with the 1UBQ X-ray structure (Vijay-Kumar, et al., *J. Mol. Biol.* **1987**, *194*, 531−544) for the protein core. However, the data are also consistent with a dynamic model of ubiquitin, exhibiting variable amplitudes, and anisotropy, of internal motions. This work suggests the possibility of primary use of residual dipolar couplings in characterizing both structure and anisotropic internal motions of proteins in the solution state.

Introduction

Over the last 5 years, the development of experimental techniques for inducing the weak alignment of macromolecules has enabled the measurement of residual dipolar couplings at a resolution and sensitivity characteristic of NMR in the solution state.[1−3] Interest has primarily centered around structural applications, because the long-range orientational constraints derived from these dipolar data nicely complement the short-range constraints typically obtained from other data such as NOEs, scalar couplings and chemical shifts.[1,3] However, the sensitivity of residual dipolar couplings to internal motions is of comparable interest.[4,5] Unlike conventional spin relaxation- and chemical exchange-based studies, residual dipolar couplings are sensitive to motions spanning a wide range of time scales and, thus, can serve as valuable probes of biologically relevant motions.[4] Although a few isolated residual dipolar coupling-based studies of dynamics in protein systems have appeared,[4,6,7] a thorough understanding of the sensitivity of dipolar coupling data to motions is yet to be established. Moreover, the interference of existing internal motions with structural interpretations of dipolar data has not been explored. Indeed, most of the existing structure refinement protocols for analyzing dipolar data implicitly assume that internal motions are either absent, negligibly small, or uniform and axially symmetric in nature.[8−11]

Here, we explore in a general way the effect of internal motions on observed residual dipolar couplings and introduce a formalism based on an order matrix analysis[12] that accomplishes a first-order separation of the effects of structure and motion. We illustrate the utility of this formalism with an application to the well-studied protein ubiquitin.[13−16] It is shown that by using an order matrix approach, accurate structural

* Corresponding author: Joel R. Tolman, Section de Chimie, BCH, Université de Lausanne, CH-1015 Lausanne, Switzerland. Telephone: ++41 21 692 3802. Fax: ++41 21 692 4035. Email: Joel.Tolman@icma.unil.ch.

† University of Toronto.

‡ Yale University.

§ University of Georgia.

|| Current address: Section de Chimie, Université de Lausanne, BCH, CH-1015 Lausanne, Switzerland..

(1) Tolman, J. R.; Flanagan, J. M.; Kennedy, M. A.; Prestegard, J. H. *Proc. Natl. Acad. Sci. U.S.A.* **1995**, *92*, 9279−9283.

(2) Prestegard, J. H. *Nat. Struct. Biol.* **1998**, *5*, 517−522.

(3) Tjandra, N.; Bax, A. *Science* **1997**, *278*, 1111−1114.

(4) Tolman, J. R.; Flanagan, J. M.; Kennedy, M. A.; Prestegard, J. H. *Nat. Struct. Biol.* **1997**, *4*, 292−297.

(5) Kay, L. E. *Nat. Struct. Biol.* **1998**, *5*, 513−517.

(6) Fischer, M. W. F.; Losonczi, J. A.; Weaver, J. L.; Prestegard, J. H. *Biochemistry* **1999**, *38*, 9013−9022.

(7) Skrynnikov, N. R.; Goto, N. K.; Yang, D. W.; Choy, W. Y.; Tolman, J. R.; Mueller, G. A.; Kay, L. E. *J. Mol. Biol.* **2000**, *295*, 1265−1273.

(8) Clore, G. M.; Gronenborn, A. M.; Bar, A. *J. Magn. Reson.* **1998**, *133*, 216−221.

(9) Clore, G. M.; Gronenborn, A. M. *Proc. Natl. Acad. Sci. U.S.A.* **1998**, *95*, 5891−5898.

(10) Clore, G. M.; Gronenborn, A. M.; Tjandra, N. *J. Magn. Reson.* **1998**, *131*, 159−162.

(11) Clore, G. M.; Garrett, D. S. *J. Am. Chem. Soc.* **1999**, *121*, 9008−9012.

(12) Saupe, A. *Angew. Chem., Int. Ed. Engl.* **1968**, *7*, 97−112.

(13) Weber, P. L.; Brown, S. C.; Mueller, L. *Biochemistry* **1987**, *26*, 7282−7290.

(14) Distefano, D. L.; Wand, A. J. *Biochemistry* **1987**, *26*, 7272−7281.

(15) Schneider, D. M.; Dellwo, M. J.; Wand, A. J. *Biochemistry* **1992**, *31*, 3645−3652.

(16) Hu, J. S.; Bax, A. *J. Am. Chem. Soc.* **1997**, *119*, 6360−6368.

10.1021/ja002500y CCC: $20.00
Published on Web 01/26/2001

parameters can often be obtained even in the presence of significant internal motions. Furthermore, it is possible to identify those regions of the protein for which the structural parameters have large potential errors. This approach suggests a route for eventually assembling a protein structure and simultaneously identifying dynamic regions of a protein, making exclusive use of dipolar coupling data.

Theory

The dipolar coupling between two spins i and j can be represented as:[12]

$$D_{ij}^{\text{res}} = -\left(\frac{\mu_0}{4\pi}\right)\frac{\gamma_i\gamma_j h}{2\pi^2 r_{ij}^3}\sum_{kl} S_{kl}\cos(\alpha_k)\cos(\alpha_l) \qquad (1)$$

where γ_i is the gyromagnetic ratio of spin i and r_{ij} is the internuclear distance between the interacting nuclei. Motion and orientation are absorbed into the order parameters S_{kl} while the fixed internal geometry is specified by direction cosines, $\cos(\alpha)$, which give the orientation of the ijth-internuclear vector relative to the three Cartesian axes of an arbitrarily chosen molecular frame. The elements S_{kl} form the order tensor, a 3×3 matrix in which only five elements are independent.[12] With sufficient independent measurements of D_{ij} for a single molecular fragment, all five of these elements can be determined.[12,17] Subsequent diagonalization of the order tensor yields a principal frame of orientation and 2 measures of order, S_{zz} and $\eta = (S_{xx} - S_{yy})/S_{zz}$. Our general approach begins by assuming that by reducing the size of the fragment, some point will be reached where the molecular fragment can realistically be assumed to be rigid. One might argue that no fragment is really rigid because of the existence of bond vibrations, but if we can assume that these fast motions can be absorbed into effective bond lengths, effectively rigid fragments can be defined. Issues relating to the determination of effective bond lengths have been addressed from both experimental[18] and theoretical[19,20] perspectives.

This sort of analysis allows different levels of ordering for different fragments and hence recognizes the possibility of internal motion; Parameters are determined describing each fragment's mean orientation *relative to the magnetic field*, plus its degree of ordering. Similar approaches have previously been used to study the conformational properties of rigid lipid[21] (or glycolipid[22,23]) subunits relative to the normal of a membrane bilayer. If the internal motions are small enough that the principal ordering axes for each fragment are dominated by the overall molecular ordering, a common overall alignment tensor must exist. Subsequent rotation of each fragment into this common frame will produce the desired mean structure. Examination of the implications of the small motion assumption and recognition of cases which violate this assumption are among the objectives in the application to ubiquitin that follows.

The principal order parameter and asymmetry parameter (S_{zz}, η) describe the orientational order of a molecular system.[12,24,25] In the absence of internal motion, these parameters will be identical for all molecular sub-fragments considered, and will reflect the overall level of alignment. In the presence of differential levels of internal motions between fragments both parameters can vary and reflect the level and character of internal motion.[4,6,7] In these situations it is quite useful to have a parameter that reflects the absolute degree of order of a specific molecular fragment (or molecule).

If we consider that the order tensor can be represented as a 5-vector consisting of averaged Wigner elements[26] then such a parameter can be defined as the Euclidean norm of this vector. We refer to this parameter, ϑ, as the generalized degree of order (GDO). It can easily be formulated in terms of Cartesian order tensor elements as follows,

$$\vartheta = \sqrt{\frac{2}{3}\sum_{ij} S_{ij}^2} \qquad (2)$$

In the case of axial symmetry of the order tensor, the GDO (ϑ) reduces to S_{zz}. We note that assuming an isotropic distribution of IS-dipolar interaction vector orientations, ϑ has a simple relationship to the standard deviation of the observed residual dipolar coupling distribution.

$$\sigma_{D^{\text{res}}} = \sqrt{\frac{1}{5}}\left|\left(\frac{\mu_0}{4\pi}\right)\frac{\gamma_i\gamma_S h}{2\pi^2 r_{\text{IS}}^3}\right|\vartheta \qquad (3)$$

The GDO is a quantity that is independent of the mean orientation of the fragment relative to the magnetic field. It is only sensitive to the extent of dynamic averaging, arising from both overall alignment effects and internal motional effects. In a sense, therefore, dynamics can be studied independently of structure, but not the converse. For purposes of discussion, it is useful to make explicit the separate contributions arising from overall alignment and from internal motion of a specific fragment. One can define a fragment specific internal GDO ($\vartheta_n(\text{int})$) as the ratio of the observed fragment GDO to the alignment tensor GDO ($\vartheta_n(\text{int}) = \vartheta_n/\vartheta_{\text{align}}$). Variations of this parameter within a set of fragments can be used to identify regions where averaging may complicate a structural interpretation.

Experimental Section

Simulations of Anisotropic Internal Motions. To examine the way in which anisotropic motion manifests itself in an order matrix approach, the effects of rotational two-site jumps were explored by computer simulation. A large set of interaction vectors is desirable in order to render the uncertainty in the order tensor determination negligible. We therefore used a real set of molecular bond vectors taken from the structural coordinates of myoglobin, a protein that has 153 NH^N interaction vectors (PDB no. 1MBC).[27] The whole molecule (which is used simply as a distribution of vectors), was used as a rigid input fragment for the simulations. Two-site jumps were carried out about a rotation axis specified in terms of polar coordinates relative to the alignment tensor PAS. Starting with a fragment expressed in the PAS of overall alignment, rotations of the molecular coordinates about a variable rotation axis by angles of $+\alpha$ and $-\alpha$ were carried out to produce two new orientations of the fragment. Note that this scheme for averaging will always preserve the "true" mean orientation of the fragment relative to alignment PAS. Residual dipolar couplings, computed for each conformer, were then averaged and the resulting

(17) Losonczi, J. A.; Andrec, M.; Fischer, M. W. F.; Prestegard, J. H. *J. Magn. Reson.* **1999**, *138*, 334−342.
(18) Ottiger, M.; Bax, A. *J. Am. Chem. Soc.* **1998**, *120*, 12334−12341.
(19) Case, D. A. *J. Biomol. NMR* **1999**, *15*, 95−102.
(20) Henry, E. R.; Szabo, A. *J. Chem. Phys.* **1985**, *82*, 4753−4761.
(21) Dufourc, E. J.; Smith, I. C. P.; Jarrell, H. C. *Chem. Phys. Lipids* **1983**, *33*, 153−177.
(22) Jarrell, H. C.; Jovall, P. A.; Giziewicz, J. B.; Turner, L. A.; Smith, I. C. P. *Biochemistry* **1987**, *26*, 1805−1811.
(23) Aubin, Y.; Ito, Y.; Paulson, J. C.; Prestegard, J. H. *Biochemistry* **1993**, *32*, 13405−13413.
(24) Sanders, C. R.; Hare, B. J.; Howard, K. P.; Prestegard, J. H. *Prog. Nucl. Magn. Reson. Spectrosc.* **1994**, *26*, 421−444.
(25) Prestegard, J. H. *Abstr. Pap. Am. Chem. Soc.* **1997**, *214*, 202-PHYS.
(26) Moltke, S.; Grzesiek, S. *J. Biomol. NMR* **1999**, *15*, 77−82.
(27) Kuriyan, J.; Wilz, S.; Karplus, M.; Petsko, G. A. *J. Mol. Biol.* **1986**, *192*, 133−154.

Table 1. Experimental Acquisition Parameters Used for Measurement of Residual Dipolar Couplings

experiment	coupling	*Nt*	nt_1	nt_2	t_1(acq)[a]	t_2(acq)[a]	duration[b]
J_{NH}-HSQC	$N-H^N$	128	76		65.516[c]		19
			82		69.892[c]		20
IPAP−HSQC	$C'-H^N$	80	200		167		21[d]
	$C'-N$						
2D HNCO	$C^\alpha-C'$	128	160		133		20
HN(CO)CA_COHA	$C'-H^\alpha$	8	48($^{13}C^\alpha$)	24(^{15}N)	40.0	22.6	25[d]
HN(CO)CA_CAHA	$C^\alpha-H^\alpha$	16	28($^{13}C^\alpha$)	20(^{15}N)	23.3	18.8	24[d]
HN(CO)CA_CACB	$C^\alpha-C^\beta$	24	42($^{13}C^\alpha$)	28(^{15}N)	28(112[e])	23.3	38

[a] In ms. [b] In h. [c] Duration of constant time evolution. [d] Includes interleaved acquisition of inphase and antiphase pathways (IPAP). [e] Effective $C^\alpha-C^\beta$ coupling evolution ($\kappa = 3.0$).

couplings (the error was set to 0.2 Hz) supplied as input for a typical order tensor determination. The output direction cosine matrix that diagonalizes the order matrix was re-parametrized into a single-axis rotation. The amplitude of this rotation was used as a measure of departure of calculated structure from the true mean structure. Programs to carry out the averaging were written in C, and simulations were carried out on an R10000 Silicon Graphics workstation. The output order tensor parameters were manipulated using the program Mathematica.

Measurement and Analysis of Dipolar Couplings in Ubiquitin. As an experimental test of our ability to detect internal motion and describe an average structure we chose to work on ubiquitin, a protein that has been well-studied by NMR.[13−16] A liquid crystalline bicelle solution[3,24] of ^{15}N,^{13}C-labeled human ubiquitin containing 15 mM phosphate buffer (pH 5.7), and 10% D_2O was prepared to a final protein concentration of 1 mM. The dilute bicelle solution (~4.5% lipid (w/v)) was prepared from fresh DHPC and DMPC with a small amount of tetradecyltrimethylammonium bromide (TTAB) added to stabilize the mixture.[28] This mixture had a final molar ratio of DHPC:DMPC:TTAB = 10:29:0.11.

All data were acquired using a Varian Inova NMR spectrometer operating at a ^1H resonance frequency of 500 MHz and equipped with a shielded, triple-resonance, single-axis gradient probehead. Coupling constant measurements were made, corresponding to seven different spin pairs along the protein backbone of ubiquitin ($N-H^N$, $C'^i-H^{N(i+1)}$, $C'^i-N^{(i+1)}$, $C^\alpha-C'$, $C'-H^\alpha$, $C^\alpha-H^\alpha$, and $C^\alpha-C^\beta$) both in the isotropic (25 °C) and the aligned (35 °C) states. Residual dipolar couplings were obtained by difference between measured couplings at each temperature. Duplicate datasets were acquired for all of the experiments to allow estimation of errors and additionally to help monitor sample stability over the course of data acquisition. Sample stability was further monitored by periodic measurement of $^1D_{N-HN}$ couplings, which can be efficiently measured with very small random errors using a HSQC experiment with phase encoding of couplings (HSQC-PEC).[29]

The $^1D_{N-HN}$ measurements subsequently used in data analysis were acquired with two modifications from the originally described HSQC-PEC experiment.[29] The first modification was the removal of the selective G^3 pulse[30] used to suppress certain systematic errors arising through cross-correlation effects. This was motivated by the reduced need for ultra-accurate coupling measurements now that much higher degrees of protein orientation can be routinely achieved and the expectation that these effects will largely cancel in taking the difference between couplings measured in the isotropic and oriented phases. The second modification was the implementation of a scheme suggested in the original work for a nearly complete removal of systematic errors arising due to differential attenuation of sine- and cosine-modulated signal pathways. This is achieved by acquisition of a pair of datasets at each temperature, differing only by appropriate choice of duration for the constant time period.[29] Measurements obtained from each dataset are averaged to obtain the final measurement.

All of the other experiments employed were frequency-based in the sense that they relied on measurement of frequency differences between multiplet components. $^1D_{C'-N}$ and $^2D_{C'-HN}$ couplings were measured simultaneously in an ECOSY fashion using the IPAP-[^{15}N,^1H]-HSQC experiment.[31,32] $^1D_{C\alpha-C'}$ couplings were measured from 2D [$^{13}C'$,$^1H^N$]-HNCO[33] datasets acquired without C^α decoupling during the C' evolution period. A 3D HNCO-based scheme[34] which utilizes the IPAP methodology[31,35,36] was used for measurement of $^1D_{C\alpha-H\alpha}$ couplings. A simple modification of this experiment allowed measurement of $^2D_{C'-H\alpha}$ couplings. In this modified version, after establishing C^α magnetization either in-phase or anti-phase with respect to H^α, magnetization was immediately transferred back to C', and then $C'-H^\alpha$ coupling evolution was allowed to proceed during the subsequent C' evolution period. A normal IPAP processing scheme allowed separation of the C' doublets into different datasets according to $^1H^\alpha$ spin state.

Finally, $^1D_{C\alpha-C\beta}$ couplings were measured using a 3D HN(CO)CA-based experiment with two notable modifications. The first modification was that single quantum C^α magnetization, anti-phase with respect to C' and N, was prepared prior to the C^α evolution period rather than $C'-C^\alpha$ multiple quantum coherence as is typically done. Second, a 400 μs C^α,C^β-selective REBURP[37] pulse was used to implement a coupling enhancement scheme[38] for acquisition of coupling information with increased efficiency. The pulse sequence used for this experiment is included in the Supporting Information. Important acquisition parameters for all of the experiments described above are summarized in Table 1. All data were processed using NMRPipe and NMRDraw software.[39] Resonance frequencies for the frequency-based experiments were determined by contour fitting using the program PIPP.[40]

Order Tensor Analyses. Order tensor analyses were carried out using the previously described singular value decomposition (SVD) implementation of the program ORDERTEN.[17] For each fragment, 10 000 error vectors were randomly sampled. The percentage of these trials which resulted in a solution which was accepted is referred to as the solution rate. Cases where the interaction vectors within a fragment are not sufficiently independent in orientation are monitored by ORDERTEN-SVD through reporting of a condition parameter. The condition parameter is the ratio of the largest singular value to the smallest, with a value of infinity corresponding to a fully underdetermined situation.

(28) Losonczi, J. A.; Prestegard, J. H. *J. Biomol. NMR* **1998**, *12*, 447−451.
(29) Tolman, J. R.; Prestegard, J. H. *J. Magn. Reson. Ser. B* **1996**, *112*, 245−252.
(30) Emsley, L.; Bodenhausen, G. *Chem. Phys. Lett.* **1990**, *165*, 469−476.
(31) Ottiger, M.; Delaglio, F.; Bax, A. *J. Magn. Reson.* **1998**, *131*, 373−378.
(32) Wang, Y.; Marquardt, J. L.; Winglfield, P.; Stahl, S. J.; Lee-Huang, S.; Torchia, D.; Bax, A. *J. Am. Chem. Soc.* **1998**, *120*, 7385−7386.
(33) Kay, L. E.; Ikura, M.; Tschudin, R.; Bax, A. *J. Magn. Reson.* **1990**, *89*, 496−514.
(34) Yang, D. W.; Tolman, J. R.; Goto, N. K.; Kay, L. E. *J. Biomol. NMR* **1998**, *12*, 325−332.
(35) Meissner, A.; Duus, J. O.; Sorensen, O. W. *J. Biomol. NMR* **1997**, *10*, 89−94.
(36) Yang, D. W.; Nagayama, K. *J. Magn. Reson., Ser. A* **1996**, *118*, 117−121.
(37) Geen, H.; Freeman, R. *J. Magn. Reson.* **1991**, *93*, 93−141.
(38) Tolman, J. R.; Prestegard, J. H. *J. Magn. Reson., Ser. B* **1996**, *112*, 269−274.
(39) Delaglio, F.; Grzesiek, S.; Vuister, G. W.; Zhu, G.; Pfeifer, J.; Bax, A. *J. Biomol. NMR* **1995**, *6*, 277−293.
(40) Garrett, D. S.; Gronenborn, A. M.; Clore, G. M. *J. Cell. Biochem.* **1995**, 71−71.

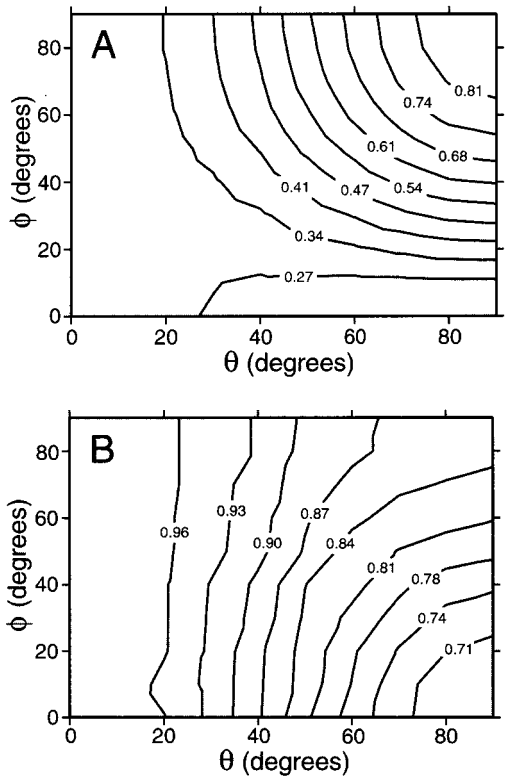

Figure 1. Contour plots illustrating the sensitivity of order tensor parameters to the spatial nature of anisotropic motions. Using the two-site jump model with fixed amplitude of ±25° to simulate anisotropic motion, resulting values for (a) the order tensor asymmetry, η and (b) the internal GDO, ϑ(int), are shown as a function of jump rotor orientation relative to the PAS of the overall alignment tensor. The asymmetry of overall alignment, η(align), was set to 0.45 for these simulations. Results for remaining regions of the unit sphere not shown can be derived from symmetry considerations.

Results

Simulations of Internal Dynamics. Although it is not possible to perform an exhaustive exploration of internal motion, it is possible to achieve a general understanding of the effects of internal motion on dipolar couplings by considering two limiting cases. These two limiting cases are isotropy of fragment motion and fluctuations in fragment orientation about a single rotator. The isotropic limit is actually trivial as it will lead to uniform scaling of all order tensor elements.[4] The other limit, which we simulate using a two-site jump, is highly anisotropic. For small jump angles (<30°), this model is effectively indistinguishable from other models involving more continuous fluctuations about a specific rotor axis. For example, the effects observed in the following cases differ only negligibly: a ±15° jump, rotations sampling a Gaussian probability distribution with $\sigma = 15°$ (e.g., the 1D GAF model[41]), or rotations sampling a uniform probability distribution bounded by ±26.2°.

Results are summarized in Figure 1 for the case of a ±25° jump about a rotor axis direction given by the polar angles θ and ϕ. Predicted values for η's range from 0.21 to 0.88 (Figure 1a) with no changes from the initial value of 0.45 when the rotator is inclined at approximately 60° to the *y*-axis. The observed changes in the GDO (Figure 1b) are also highly dependent on the orientation of the rotator relative to the overall alignment frame. For a jump amplitude of ±25°, the reduction in the GDO ranges from a factor of 0.98 to 0.68. The minimum reduction from the initial value of 1.0 occurs in the case of an internal rotator axis coincident with the alignment tensor *z*-axis. A rotator coincident with the *x*-axis of the alignment tensor ($\phi = 0$, $\theta = 90$, the direction of lowest order) produces the maximum reduction. Results for S_{zz} are similar to those for the GDO but display a more limited sensitivity to internal motion, the extent of which depends strongly on the asymmetry of overall alignment.

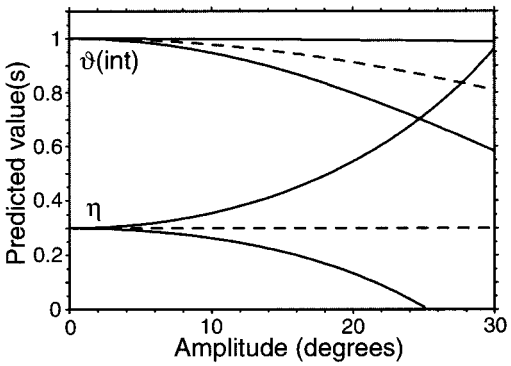

Figure 2. Predicted ranges of ϑ(int) and η resulting from internal motions modeled both as isotropic and using the two-site jump model. The effects of isotropic internal motions (dashed lines) are described via diffusion within a cone of any constitutive vector of the fragment with the amplitude corresponding to the cone semiangle. For anisotropic (two-site jump) motions, a range of values result from any single amplitude due to the dependence on the orientation of the rotor relative to the alignment frame. These ranges are delimited by solid lines. The ranges shown are specific for an asymmetry of overall alignment corresponding to that observed for ubiquitin ($\eta = 0.30$) in the current study.

Shown in Figure 2 are predicted ranges of ϑ(int) and η expected to result from internal motions of variable amplitude, both for isotropic internal motion as well as two-site jumps. Although the results shown are specific for η(align) = 0.30, predicted dispersion in values of the GDO and η are nearly independent of overall alignment asymmetry. It is important to recognize that *for anisotropic internal motions, the GDO does not reflect an amplitude of internal motion but rather a combination of amplitude and direction*. On the other hand, for isotropic internal motions ϑ(int) is formally equivalent to axially symmetric averaging of all constitutive vectors within the fragment, described by an associated order parameter S.

Accuracy of Structural Information in the Presence of Internal Motions. The primary issue for structural accuracy is the validity of reassembling fragments on the basis of the assumption that their respective ordering PASs remain coincident. In the simplest case, in which individual molecular fragments exhibit only very small internal fluctuations, it can be expected that each fragment's degree and direction of ordering will primarily be dictated by the overall aligning mechanism and internal motion will have minimal effects on determined order tensor parameters. Another simple case also results when internal motions are of greater amplitude, but are isotropic in nature; that is, the degree of motional averaging which occurs due to internal motion of the fragment is uniform in all directions. In this case the internal motion uniformly scales down measured residual dipolar couplings, and hence the direction of order for that fragment is dictated solely by the overall alignment of the protein.

Departure from isotropy of internal motion is therefore the case of primary concern. We again return to the two-site jump model as a limiting case for such anisotropic motion. A range of amplitudes and rotation axis orientations were explored using

(41) Bruschweiler, R.; Case, D. A. *J. Am. Chem. Soc.* **1994**, *116*, 11199−11200.

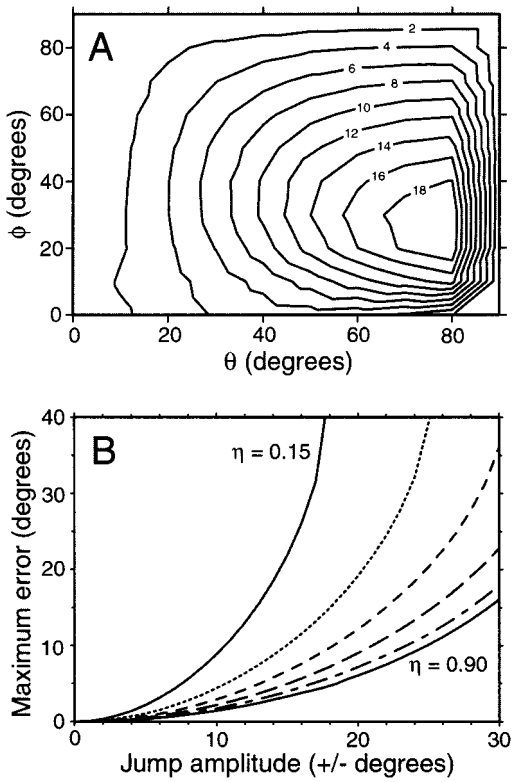

Figure 3. Plots depicting the predicted errors ω (in degrees) arising from an order tensor-based structural analysis that assumes coincidence of fragment and global alignment PAS orientations. These errors are the result of internal motion, modeled here using angular two-site jumps. The angular errors cited were taken as the magnitude of the single rotation that carried the PAS of the solution order tensor into the reference global alignment frame. (a) For a jump amplitude of $\pm 25°$, the expected error ω is plotted as a function of the polar angles, θ and ϕ, describing the position of the rotor-axis relative to the principal axis system of an overall alignment tensor. The overall alignment tensor was assumed to have an asymmetry corresponding to $\eta = 0.45$. (b) Dependence of the maximum predicted error (ω_{max}) on jump amplitude and alignment tensor asymmetry. Each curve corresponds to a different alignment asymmetry, incremented in steps of 0.15.

this jump model. As we previously mentioned, we model these jumps symmetrically such that the mean orientation of the rigid fragment is preserved when the two states are equally populated. Subsequent order tensor analysis of the calculated average couplings then allows straightforward determination of the "experimental" PAS. The deviation from the starting reference PAS is then quantitated by computing the unique angle, ω, corresponding to the single rotation that transforms one frame into the other. In the case that motion does not have an effect on the mean structure, the experimentally determined PAS remains coincident with the original reference PAS. Deviation of these two PAS frames thus corresponds to the accuracy with which this method can reproduce a mean structure when anisotropic motions of this sort are present.

Results for internal fragment jumps of $\pm 25°$, and using an overall alignment tensor asymmetry of $\eta = 0.45$, are shown in Figure 3a. It is clear that deviations can exist and that they vary depending on the position of rotor axis relative to the PAS of the alignment tensor. Note that when the rotor axis coincides with one of the principal axes of the alignment tensor ($\theta = 0°$, or $\theta = 90°$ and $\phi = 0°$ or 90°), no error is introduced. The maximum effect produced in this case occurs for rotor axes in the region of the unit sphere described by the polar angles (80°, 40°), for which an error of 20° is predicted. We note that the

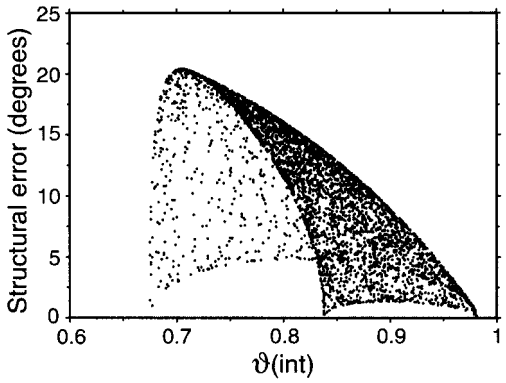

Figure 4. Theoretical correlation plot relating the internal GDO, ϑ(int), to predicted structural errors, ω, using the rotational jump model of amplitude $\pm 25°$. Each point represents the simulated result arising from a single rotor orientation relative to a global alignment frame with asymmetry $\eta = 0.45$, with rotor orientations sampled randomly over the entire unit sphere. It is apparent that the magnitude of *potential* structural errors in an order tensor approach correlate well with an observed reduction in the value of the GDO.

error is not uniformly distributed. For example, in the case discussed above, the maximum error in orientation for the *z* axis is 4.8° with a mean error (over all rotation axis positions) of 1.8° and a standard deviation of 1.5°, while the maximum error for the *x*-axis is 19.7° with a mean error of 5.4° and standard deviation of 5.8°. While most of the structural errors are small, it is clear that there is an approximate threshold amplitude, above which deviations can quickly become very large (see Figure 3b). Moreover, use of an aligning medium with high asymmetry reduces the magnitude of deviations, primarily due to improved sensitivity to orientation of the *x* and *y* axes.

It is of interest to be able to identify cases where motions exceed this threshold and where structural parameters may be unreliable. The values for ϑ (and by extension ϑ(int)) reflect the degree to which internal motions have averaged the observed dipolar couplings. The GDO can, therefore, be used to identify fragments that are particularly susceptible to errors in an order tensor-based structural analysis. Figure 4 shows the correlation between ϑ(int) and the computed structural error on the basis of our simulated results for the $\pm 25°$ jump. As can be seen, observation of a high relative ϑ(int) implies that the resulting ordering PAS has not been corrupted by the presence of motion. In this case, ϑ(int) > 0.95 suggests that the deviation in axis orientation is less than 4° (i.e., $\omega < 4°$). On the other hand, a relatively low ϑ(int) serves to warn of the possibility of error in the structural analysis.

Application to Ubiquitin. To illustrate this approach to the analysis of residual dipolar couplings, dipolar coupling measurements were made corresponding to seven different interactions along the peptide backbone of ubiquitin ($^1D_{C\alpha-C\beta}$, $^1D_{C\alpha-C'}$, $^1D_{C\alpha-H\alpha}$, $^2D_{C'-H\alpha}$, $^1D_{C'-N}$, $^2D_{C'-HN}$, and $^1D_{N-HN}$ couplings). Analysis of a mixture of data originating from multiple dipolar interaction types requires some knowledge of the relative effective internuclear distances operative for the different interactions.[18−20] To approximately account for these relative differences in effective bond distances, a nonlinear least-squares fit of overall order tensor magnitude and orientation to each of the seven sets of dipolar coupling measurements was carried out using the X-ray coordinates of ubiquitin (1UBQ).[42] Excluded from the fits were measurements corresponding to residues 32

(42) Vijaykumar, S.; Bugg, C. E.; Cook, W. J. *J. Mol. Biol.* **1987**, *194*, 531−544.

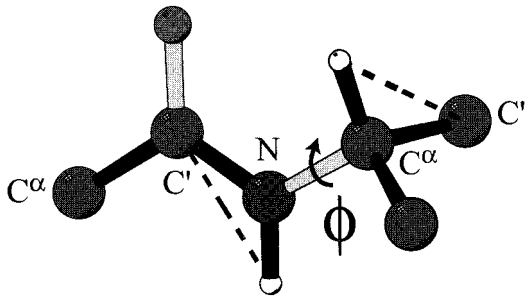

Figure 5. The rigid peptide fragment utilized in the analysis of the experimental ubiquitin data. Available dipolar coupling measurements between directly bonded nuclei are indicated by dark bonds, while dashed lines indicate measurements between nonbonded nuclei. The geometry of the fragments was taken directly from the ubiquitin PDB coordinates (1UBQ). Fragments were numbered according to the residue number of the C^{α} nucleus central to the fragment.

and 48, which were consistent outliers for a majority of the seven sets considered, and measurements corresponding to C-terminal residues 71−76, which exhibit particularly low spin-relaxation derived order parameters[15,43] and high *B*-factors.[42] This procedure is similar to that adopted in the work of Ottiger and Bax,[18] except that the fit was performed independently for each set of measurements. The fitted values for S_{zz} were used to deduce effective values of pairwise distances using a $C^{\alpha}-C'$ bond length of 1.525 as a reference.[18,44]

Using all of the data and effective distances, the alignment tensor orientation is described by the Euler angles ($\alpha = 38°$, $\beta = 34°$, $\gamma = 30°$), relative to the native 1UBQ reference frame. The resulting asymmetry parameter, η, was 0.30 and the global value for S_{zz} was 7.63e − 4 ($\vartheta_{\text{align}} = 7.74\text{e} - 4$). The rmsd's between measured and best fit predicted dipolar couplings were 0.43, 0.30, 2.7, 0.58, 0.23, 0.59, and 1.2 Hz, respectively, for $^1D_{C\alpha-C\beta}$, $^1D_{C\alpha-C'}$, $^1D_{C\alpha-H\alpha}$, $^2D_{C'-H\alpha}$, $^1D_{C'-N}$, $^2D_{C'-HN}$, and $^1D_{N-HN}$ couplings. In all cases the rmsd is significantly larger than experimental error (0.11, 0.14, 1.0, 0.26, 0.13, 0.33, and 0.20 Hz, respectively), suggesting deviation due to minor structural variations or internal motion.

Fragment-by-Fragment Analysis. Measurements were grouped into sets corresponding to peptide backbone fragments containing the C^{α} atom, its four directly bonded atoms and the adjacent peptide plane containing the carbonyl C($i - 1$) atom. Note that the defined fragments include one torsional degree of freedom (the backbone torsion ϕ), which was initially set according to the X-ray coordinates. Figure 5 illustrates the structure of the fragments employed. A maximum of eight measurements per fragment was thus obtained. In addition to the dipolar coupling measurements, necessary input information includes the estimated errors of measurement, the effective bond distances, and the polar angles of the relevant interaction vectors relative to some fragment-fixed frame. In our case, the 1UBQ coordinates of ubiquitin,[42] transformed into the global alignment PAS resulting from the combined fit described above, were used directly to obtain the starting vector orientations. Insisting that at least six dipolar coupling measurements be available per fragment, 45 such fragments of ubiquitin could be considered. Motivated partially by the fact that our fragments contain a single torsional degree of freedom, we chose a working uncertainty at 1.5 times the estimated experimental uncertainty (1.5σ). Using the program ORDERTEN-SVD, an acceptable solution rate (>2%) was obtained for 24 of the original 45 fragments. Similar results are obtained if coordinates from a second X-ray structure (1UBI),[45] or any of the 10 available NMR structures (1D3Z)[46] are used. In the case of the 1UBI structure, only fragment 20 (3% solution rate) could be added to the acceptable solution list (see Figure 6 below). Results are consistent among the group of NMR structures, with addition of fragments 20, 48, and 60 to the acceptable solution list, and deletion of fragments 7, 25, 59, and 66.

For cases where solutions were found, the fragment-specific alignment frames can be compared to the global alignment frame as an indication of structural deviation. In Figure 6, considering the entire space of acceptable solutions, the minimum observed angular deviation between derived fragment and global alignment PAS orientations are plotted as a function of fragment number. From this plot, it is apparent that most of the fragments considered have acceptable orientational solutions that are highly consistent (<6°) with expectations based on the 1UBQ X-ray coordinates.[42] Fragments that exhibit notable deviations fall in three separate regions, residues 6−11, 39−42, and the C-terminal tail (residues 71−76).

A summary of the resulting values for the GDO are presented in Figure 7. Shown are the mean and standard deviation of the distribution of ϑ obtained for each fragment. Also shown are values of ϑ corresponding to the solution of minimum angular deviation from the reference, which complement the results presented in Figure 6. Overall it is apparent that, corresponding to cases of minimum orientational deviation from the X-ray structure, there is a core range for ϑ, which runs approximately from 0.0007 to 0.0009. Fragments 40 and 74 (which exhibit structural deviations from the X-ray reference structure) as well as fragment 57 exhibit a GDO that is notably lower than this range. Hence, structural deviations should be discounted for these residues. Note that fragments 40 and 57 lie in regions of transition between secondary structural elements and fragment 74 lies in the highly mobile C-terminal tail.

Fragment 68 has an unrealistically high GDO. The range of ϑ obtained for fragment 68 is also the largest. This along with warning about underdetermination from the ORDERTEN program indicates that there are additional factors to consider. A closer look reveals that three of the six measurements employed for this fragment correspond to interactions which, relative to the fitted global alignment frame, are quite close to the magic angle and thus have quite small measured dipolar couplings. While these small numbers are useful in the determination of orientation, they do not help in the determination of degree of ordering of the fragment. Hence we discount this point.

Refinement of ϕ. It is significant that ~40% of the fragments initially considered either gave no solutions at all or only a very small number of solutions. This suggests strongly that our initial assumptions concerning fragment geometry or fragment rigidity may be inadequate. The most obvious source of error in the current analysis centers around the inclusion of the backbone dihedral angle ϕ within the fragment definition. Static differences between solid-state and solution-state values for this angle as well as motional averaging about this angle could lead to the observed absence of order tensor solutions. One possible way to address structural deviations is to use ϕ values determined from NMR *J*-coupling measurements in solution.[47]

(43) Tjandra, N.; Feller, S. E.; Pastor, R. W.; Bax, A. *J. Am. Chem. Soc.* **1995**, *117*, 12562−12566.
(44) Engh, R. A.; Huber, R. *Acta Crystallogr., Sect. A* **1991**, *47*, 392−400.
(45) Ramage, R.; Green, J.; Muir, T. W.; Ogunjobi, O. M.; Love, S.; Shaw, K. *Biochem. J.* **1994**, *299*, 151−158.
(46) Cornilescu, G.; Marquardt, J. L.; Ottiger, M.; Bax, A. *J. Am. Chem. Soc.* **1998**, *120*, 6836−6837.
(47) Wang, A. C.; Bax, A. *J. Am. Chem. Soc.* **1996**, *118*, 2483−2494.

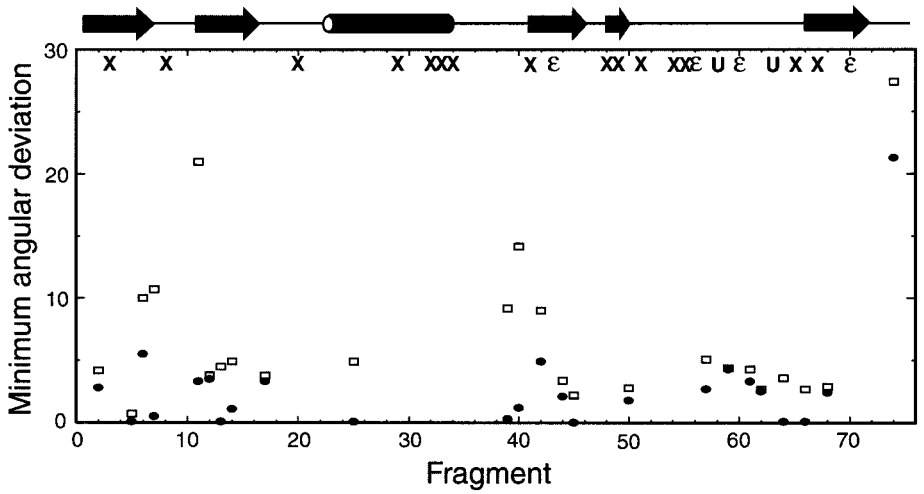

Figure 6. Minimum acceptable angular deviations using the best fit global alignment tensor to the 1UBQ coordinates as reference. Total angular deviations, which correspond to ω, (open squares) and the angular deviation observed for the principal axis (z, filled circles) are shown. Fragments excluded from consideration are indicated according to their reason for exclusion: No solutions (**X**), < 2% solution rate (ϵ), or a condition number > 25 (**U**).

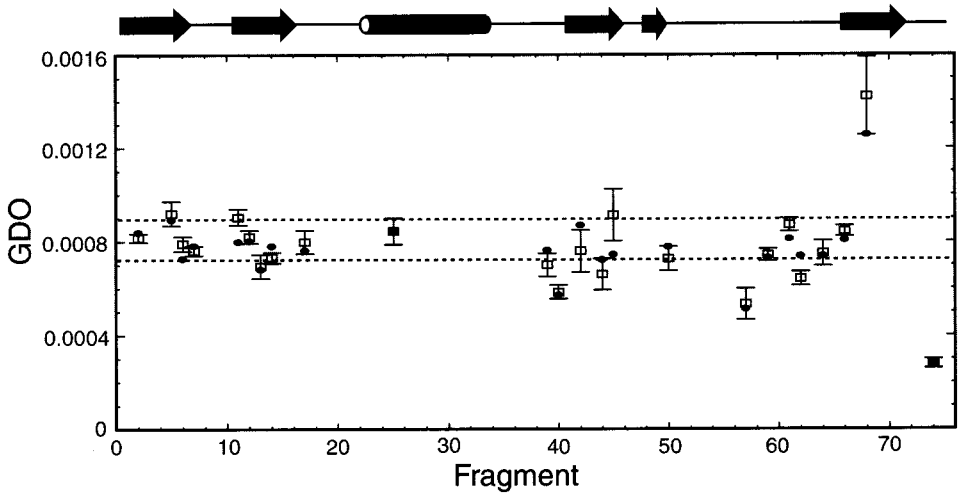

Figure 7. Summary of acceptable values for the GDO, ϑ, as a function of fragment number. The mean and standard deviation of the distribution of ϑ for each fragment are denoted by open squares and corresponding error bars, respectively. The filled circles denote the value of the GDO observed for the solution of minimum angular deviation from the X-ray reference frame. The dotted lines denote an approximate core range of these values, for purposes of later discussion.

Among the set of fragments considered, these refined values of ϕ represent deviations from the 1UBQ values ranging from −13.8° to +15.3°. These modifications were carried out by a rotation of the peptide plane, while preserving the orientation of the C^{α} group relative to the reference coordinate axes. While acceptable solutions were obtained in the cases of fragments 34, 48, and 60, use of the refined values for ϕ led to a loss of acceptable solutions for fragments 59 and 66. For the 15 fragments that exhibited no solutions using the 1UBQ X-ray geometry, we tried a systematic search for values of ϕ that could lead to a solution space within our acceptance criterion of >2%. In this study, 4 fragments yielded acceptable solution rates upon modification of ϕ by <20°, but satisfactory explanations for the remaining 11 could not be obtained. Five of the fragments (32, 33, 41, 49, and 67) required rather large modifications of ϕ (at least 25−50°), while the other six yielded no solutions (3, 8, 51, and 54), or a negligibly small number (<0.1% for 20 and 55) regardless of the value of ϕ. We cannot entirely exclude other explanations at this point, such as significant deviations of bond lengths and angles beyond those encompassed by the solid- and solution-state coordinates employed in the analysis. However, the fact that these "bad" 11 fragments are largely clustered and lie in or adjacent to regions exhibiting large *B*-factors (8−10, 31−34, 50−55) suggests that they may undergo conformational averaging about ϕ to an extent that makes our assumption of fragment rigidity untenable.

Motional Models for Interpretation. While we cannot reach truly definitive conclusions about motion at sites that fail to yield order tensor solutions, we can be more specific about smaller amplitude motions of those fragments for which we have solutions, and for which variations in GDOs are modest (excluding fragments 13, 40, 57, 68, and 74). Using the observed upper limit GDO value as the reference value for minimum averaging, an estimate of ϑ(int) for each fragment is computed simply from the ratio of observed GDO to this reference. In this case, we obtain variations in ϑ(int) from 0.81 to 1.0. We consider two simple limiting cases in seeking a physical picture of motion that can give rise to a reduction in ϑ(int) to 0.81. The first model we employ is one in which all internal motions are purely isotropic in nature (same limited degree of averaging

(48) Wand, A. J.; Urbauer, J. L.; McEvoy, R. P.; Bieber, R. J. *Biochemistry* **1996**, *35*, 6116−6125.

about three orthogonal axes). Within the context of this model, the GDO has a direct correspondence with motional amplitude (Figure 2). It indicates a variable level of internal motion, ranging from cone semiangles of 0° to 30°, applicable to all interaction vectors within a given fragment. Consideration of error bars in Figure 7 reduces this range somewhat, but variations are nevertheless significant. We also consider an anisotropic two-site jump model, employed earlier for simulations. In this case observed reductions in the GDO do not necessarily correlate directly with motional amplitude because it is also highly sensitive to the position of the rotor axis relative to the PAS of the alignment tensor. If we ascribe variations in ϑ(int) as arising purely from variations in rotor orientation, then a uniform jump amplitude of ~19° would be consistent with our results (Figure 2).

We now note that one can distinguish between isotropic and anisotropic motional models by considering values for the asymmetry parameter, η. Variations in this parameter between fragments are indicative of anisotropic motion. The core set of values obtained for η, corresponding to orientational solutions most consistent with the X-ray structure, span a range from 0.18 to 0.53, with the best fit alignment tensor value lying at 0.30. This variation suggests the presence of anisotropic motion. These η variations are also well reproduced with 17−19° jump amplitude which was independently suggested by the ϑ(int) data. One must be cautious however in that η values are the among the least well determined parameter in the analysis.

Discussion

Residual Dipolar Couplings as Motional Probes. Several points can be drawn from the results of our simulations regarding the sensitivity of residual dipolar couplings to internal motions. Regardless of the specific model employed, motions of very small amplitude (<10°) have very little influence on observed residual dipolar couplings. However, this sensitivity increases rapidly thereafter, and for amplitudes greater than 15°, motional effects can be observed. It is likely that many motions of functional significance have amplitudes equal to or greater than 15°. Our results on ubiquitin suggest that some motions are well into the range of observability. Detection of these motions is not always straightforward, and in cases of high anisotropy they are not universally reflected in specific dipolar couplings or S_{zz}. The generalized degree of order derived here gives a better indication, but ultimately the acquisition of residual dipolar couplings using multiple alignment media may be the best route for detecting these motions.

A First-Order Separation of Structure and Dynamics. One of the primary goals of this study is to determine the effect of motion on the accuracy of structure determination. In general, when using an order tensor analysis these effects depend on both the amplitude and extent of anisotropy of motion, but they are often small. In the worst case, for systems oriented with an intermediate degree of asymmetry ($\eta = 0.45$), and having highly anisotropic motions (e.g., two-state jump) of moderate amplitudes (25°), errors in extracted structural parameters are no more than 20° (i.e., ω < 20°). As was shown (Figure 3b), these potential structural errors are quite dependent on the asymmetry parameter of the global alignment tensor, with higher asymmetry parameters affording a more robust extraction of structural parameters. Hence, a crude separation of motion and structure is possible.

For ubiquitin, motions are of small to moderate amplitude within the protein core, and we expect that structural information can be extracted with reasonable accuracy using an order tensor approach. When motions are small enough, effects of motion can be absorbed into the determined order parameters, leaving structural parameters largely intact. This represents a considerable advantage relative to simulated annealing approaches that assume a global set of order parameters and thus absorb even small motional effects into structural parameters.

In cases where motional contributions are large, the presented formalism can still provide a level of filtering. In particular, the GDO parameter allows a direct assessment of the extent to which couplings have been motionally averaged. In practice, regions of the molecule with significantly small GDO parameters warrant careful consideration during structure calculation. In this study, fragments 40, 57, and 74 are clearly three cases that fall into this category. We are encouraged by the fact that with only a few exceptions, the results for ubiquitin presented here suggest a solution-state structure that is in very good agreement with the 1UBQ X-ray structure. It suggests that it may be possible to obtain structures of moderate resolution from dipolar coupling data alone using just the first-order separation of internal motions which was employed here.

Local Fragment Geometry. This sort of order tensor analysis assumes that one is working with rigid fragments of known molecular geometry. In our application to ubiquitin, we chose to work with very small fragments so as to reduce assumptions about fragment geometry. Even though our fragments were small, consisting of a peptide plane in addition to a C^{α} carbon, specific cases were encountered where few or no order tensor solutions were obtained. We believe the inclusion of a dihedral ϕ, having dynamic averaging or static deviations from structural coordinates within our fragment, to be the most likely cause. The lack of improvement obtained using NMR scalar coupling-refined values for the dihedral ϕ[47] suggests that at least some dynamic component is required. Although errors in other assumed geometrical parameters could in principle explain these cases, given that our inherent precision of determination of fragment orientation relative to the alignment tensor principal axis is usually at least ±5°, these deviations would in many cases need to be unrealistically large. To see this we note that the observed set of solutions for a given fragment is the intersection of the allowed solutions for each of the constitutive vectors. Thus, starting from a perfect geometry and neglecting compensatory effects due to corresponding changes in estimated order parameters, one might roughly estimate that a change on the order of 10° in the relative orientation of a pair of vectors would be required to make the intersection vanish. The difficulty in achieving such a geometry without excessive departures from ideality is supported by the fact that very similar results were observed using the NMR-derived coordinates.[46] This particular ensemble of structures was refined against bicelle-induced dipolar couplings very similar to those used in the current study, and thus one might expect that any satisfactory explanation, based on deviation from an assumed rigid fragment geometry, would have been found.

Structure and Dynamics of Ubiquitin. Despite the fact that the data above are, in large part, highly consistent with the static 1UBQ X-ray structure, there are a few specific regions of the protein that seem to exhibit a significant level of variation. Among these is the region surrounding the loops spanning residues 8−11 and residues 39−42, which constitute a region of transition between loop and β-strand, and the C-terminal tail. Both residues 40 and 74 have low GDO values, suggesting that some apparent structural variation involving these residues might be an artifact of motion. Interestingly, residues near the start of the C-terminal tail are in spatial proximity to residues 41−42.

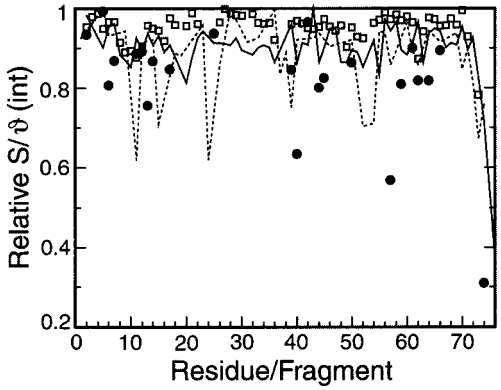

Figure 8. Comparison of ϑ(int) (filled circles) with spin relaxation derived order parameters. Shown are S_{NH} order parameters reported by Tjandra et al.[43] (open squares) and Schneider et al.[15] (solid line), as well as $S_{C\alpha H\alpha}$ order parameters reported by Wand, et al.[48] (dotted line). Values of ϑ(int) were those corresponding to solutions of minimum orientational deviation from the 1UBQ X-ray structure. Within each set, all values were scaled relative to the largest ϑ (or S) observed.

In addition, the data point to several departures from our normal static view of the ubiquitin structure. In the limiting case that internal motions are isotropic, a direct comparison of ϑ(int) and spin relaxation order parameters, S, is meaningful (Figure 8). For this limiting case, the dipolar coupling data indicates greater variations and modestly larger amplitudes than the spin relaxation data. We note that there is no apparent correlation between them, except for the reduction at the C-terminal residues. These observations could be due to the different time scale sensitivities of the two, or alternatively the motions may be significantly anisotropic. If motions are anisotropic, it remains that a number of fragments must exhibit amplitude of motion larger than expected based on the spin relaxation data. For fragments 40 and 57 fairly large motional amplitudes are required to explain the observed GDO. For a two-site jump, a minimum amplitude of approximately $\pm 30°$ is required. The required amplitude is even larger if motions are assumed to be closer to the isotropic limit.

Some conclusion might also be drawn from fragments that display very few or no acceptable solutions using the order tensor approach. We observe that nine of these 15 fragments lie within two distinct regions (29−34 and 48−55), that correspond to regions exhibiting very high *B*-factors in both the 1UBQ and 1UBI X-ray structures. Of the remaining six, three lie in loops (fragments 8, 20, and 65), and two, on the edge of secondary structural elements (41 and 67). It is not unreasonable that these fragments exhibit some level of conformational variability. The possibility of screening a protein based on incompatibility with a rigid model may have some important implications for the study of functional dynamics.

Concluding Remarks

Current protocols for biomolecular structure determination by NMR center around the characterization of a single model, with assumptions concerning the nature and extent of internal motions made to reduce the number of degrees of freedom. Although structures can now be determined with high precision, it remains difficult to assess their accuracy. It is clear that the presence of internal motions of sufficient amplitude can compromise the accuracy of the final structure. The current work investigates the possibility of including some internal mobility in the model, based on the assumption that the local geometry is known. While this approach can in principle improve accuracy, based on the level of agreement with the dipolar data, it comes at the cost of lower precision.

The fact that a similar set of dipolar couplings was employed, but in a very different fashion, during the refinement of the NMR structure was a primary motivation for the use of the X-ray structure as a reference structure in this work. Nevertheless, the results of this analysis obtained using the NMR coordinates (1D3Z)[46] indicate a comparable or slightly better level of structural consistency relative to the 1UBQ coordinates, with a similar distribution of GDOs. This is not very surprising given our relatively low level of precision and the fact that the two structures are in agreement with a backbone rmsd of 0.4 Å. The present analysis can only resolve larger deviations between the two structures. On the other hand, the approach still indicates specific regions within ubiquitin, rather consistently across all reference structures employed, which certainly merit further consideration. Such consideration awaits further information, perhaps in the form of bonding constraints between fragments or data acquired in additional alignment media.

Acknowledgment. This work was supported by the Human Frontiers Science Program Organization (J.R.T.), a Grant from the Natural Science and Engineering Research Council of Canada (L.E.K.), and a Grant from the National Science Foundation of the United States, MCB 9726344 (J.H.P. and H.M.A.). L.E.K. is a foreign investigator of the Howard Hughes Medical Research Institute. We thank Professor J. Wand for providing the sample of ubiquitin used in this study and Daiwen Yang for measuring the $^1D_{C\alpha-H\alpha}$ and $^2D_{C'-H\alpha}$ couplings. We thank Nikolai Skrynnikov and Mark Fischer for their useful insights at several stages during the development of this work.

Supporting Information Available: A diagram of the pulse sequence employed for the measurement of $^1D_{C\alpha-C\beta}$ couplings; two figures summarizing results obtained using model 1 of the 1D3Z structure as reference (PDF). This material is available free of charge via the Internet at http://pubs.acs.org.

JA002500Y